

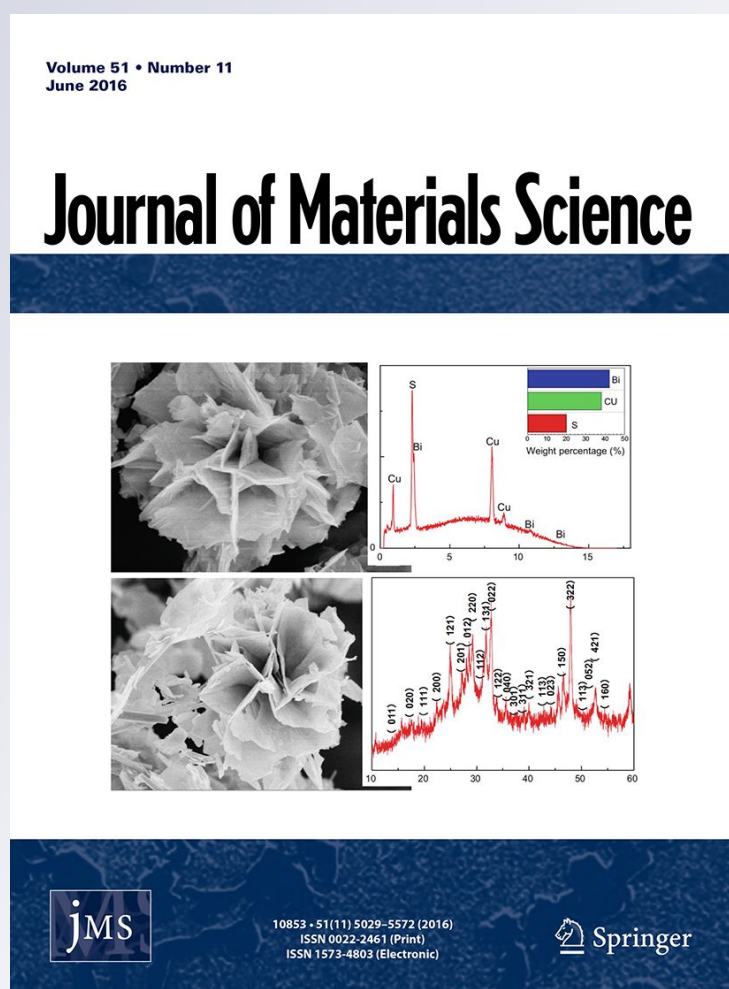
Separation of perchlorates from aqueous solution using functionalized graphene oxide nanosheets: a computational study

Pariza Ansari, Jafar Azamat & Alireza Khataee

Journal of Materials Science
Full Set - Includes 'Journal of Materials
Science Letters'

ISSN 0022-2461
Volume 54
Number 3




J Mater Sci (2019) 54:2289-2299
DOI 10.1007/s10853-018-3045-2



Your article is protected by copyright and all rights are held exclusively by Springer Science+Business Media, LLC, part of Springer Nature. This e-offprint is for personal use only and shall not be self-archived in electronic repositories. If you wish to self-archive your article, please use the accepted manuscript version for posting on your own website. You may further deposit the accepted manuscript version in any repository, provided it is only made publicly available 12 months after official publication or later and provided acknowledgement is given to the original source of publication and a link is inserted to the published article on Springer's website. The link must be accompanied by the following text: "The final publication is available at link.springer.com".



Separation of perchlorates from aqueous solution using functionalized graphene oxide nanosheets: a computational study

Pariza Ansari¹ , Jafar Azamat² , and Alireza Khataee^{1,3,*} 

¹Research Laboratory of Advanced Water and Wastewater Treatment Processes, Department of Applied Chemistry, Faculty of Chemistry, University of Tabriz, 51666-16471 Tabriz, Iran

²Department of Basic Sciences, Farhangian University, Tabriz, Iran

³Department of Materials Science and Nanotechnology Engineering, Faculty of Engineering, Near East University, 99138 Nicosia, Mersin 10, Turkey

Received: 8 July 2018

Accepted: 18 October 2018

Published online:
29 October 2018

© Springer Science+Business Media, LLC, part of Springer Nature 2018

ABSTRACT

In this research, separation of perchlorate ion from aqueous solutions is investigated using functionalized graphene oxide nanosheet (GONS) membrane. Due to the ultrathin thickness of GONS, it was expected to have good water permeability of this membrane. At the same time, for the water treatment, it is necessary for perchlorate ions to stay behind the membrane, and to achieve this, appropriate pores with the functionalized groups at their edge should be created on the surface of GONS, so that the water molecules pass through them and the considered ions do not pass. The investigated systems included three types of functionalized GONS immersed in an aqueous solution of sodium perchlorate. Three different functional groups (–F, –OH and –H) were used on the edge pore with various sizes, and an external pressure was applied to the systems for permeation of water molecules through pores. The results showed that the GONS with a suitable functionalized pore was impermeable to perchlorate ions with a high permeability for water molecules.

Introduction

Today, due to the changing lifestyle of humans, industrial development and energy demand, the water scarcity has become a serious problem [1]. The lack of attention from human societies, as well as the increase in the industrial chemicals, agricultural and commercial materials, causes wastewater to be

poured into rivers. So, environment and source of drinking water are infected [2]. Water pollutants include toxic heavy metals, nitrate ions, cyanides, perchlorates, trihalomethanes and organic pesticides. These pollutants have an important effect on the immune system and expression of immune-related genes [3].

Address correspondence to E-mail: a_khataee@tabrizu.ac.ir

In the meantime, perchlorate ion is one of the major contaminants in drinking water in the form of perchloric acid, ammonium perchlorate, potassium perchlorate and sodium perchlorate [4]. Perchlorate ions as the water contamination have high mobility, high stability and non-reactive nature; therefore, removal of this contamination from aqueous solution is important [5]. Perchlorate as a chlorinated compound in water is a strong oxidizing agent and highly soluble and stable in water. The most important adverse health effects of perchlorate in the low doses are similar to those that are caused by iodine deficiency. Also, perchlorate at the high doses causes adverse health effects such as impaired blood circulation. Therefore, it is necessary to use some methods that can reduce its condensation in water [6].

Various purification methods are used for wastewater purification, such as distillation [7], electrolysis [8], adsorption [9], ionic exchange method [10], reverse osmosis [11], chemical processes [12] and nanostructure membranes filtration [13]. Use of nanostructure membranes is preferable because of lower energy consumption, high selectivity and continuous performance [14]. These membranes play an important role in the application of molecular separation, DNA sequencing, drug release and biosensing. Nanostructure membranes made of polymeric materials have great application in the molecule separation due to their adjustable size and molecule selectivity. However, the controlling ability of the aperture shape or dimension is usually restricted by a template-mediated approach [15]. Some nanostructure membranes such as carbon nanotube [16], boron nitride nanotube [17], boron nitride nanosheet [17], graphene [18–20] and graphene oxide nanosheets (GONSs) [21, 22] are used for filtration of wastewater. In these membranes, mostly water molecules pass through the membrane and the pollutants stay behind the membrane.

In this regard, water transport across graphene-based membranes, because of its ability in filtration process and separation technology, has attracted much attention [23, 24]. GONS is an exciting material for its possible applications [25], including protective layer, ion conductor, material for molecular storage and water purification. GONS is produced by adding epoxy and hydroxyl groups to graphene surface with different percentages. These functional groups could be randomly distributed on both sides of the GONS [26]. To use GONS in water purification process, this

membrane should have some pores on its surface. Via a thermal reduction process, the intrinsic defects in GONS are caused, resulting in nanopores formed with a variety of sizes [27]. Chiang et al., by creating some defects in reduced graphene oxide, produced some pores with different sizes on its surface. Reduced graphene oxide membrane can be used for separation processes [28]. Wei et al. studied the water permeation through GONS by considering water flow through the interlayer membrane and pores on the surface of membrane. They concluded that the transport of water between the graphene plates was faster because of the reduced friction at the interface of solid–liquid [29].

In this work, we investigate the separation capability of functionalized GONS membrane for removal of perchlorate ions from aqueous solution by molecular dynamics (MD) simulations technique. For this, we designed some GONS membranes with various functionalized pores on their surfaces to investigate their effects on the separation of perchlorate ions from water. The fabrication of functionalized nanostructure membranes takes place slowly. So, it is better to design the new membranes by computational methods. With the development of computer science, computational methods have become a promising tool to provide molecular insight into physical chemistry phenomenon [30]. In this regard, MD simulations provide an important complement to experimental and theoretical analyses and system properties can be easily obtained [31]. This method is a powerful computational method based on the Newton's equations, so that the macroscopic properties of the system can be obtained from its microscopic properties using statistical mechanics [32].

Computational methods and details

In this research, we designed various GONS membranes with the three different functional groups including $-F$, $-OH$ and $-H$ on the edge pores, namely F-pore, OH-pore (hydrophilic pores) and H-pore (hydrophobic pore) systems to investigate the removal of perchlorate from water as shown in Fig. 1. The pore size was measured by showing atoms as van der Waals spheres and calculating the amount of area not filled by any atomic representations. The area of pores was 14.65 \AA^2 , 17.04 \AA^2 and 24.84 \AA^2 for F-pore, OH-pore and H-pore systems, respectively. In

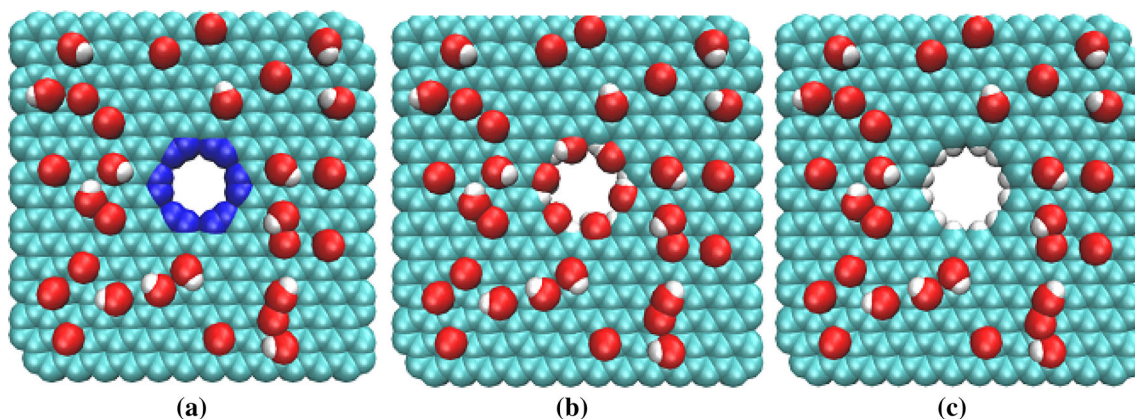


Figure 1 Different pore architectures of GONS; **a** F-pore (pore area: 14.65 \AA^2), **b** OH-pore (pore area: 17.04 \AA^2) and **c** H-pore (pore area: 24.84 \AA^2) (cyan: carbon, red: oxygen, white: hydrogen and blue: fluorine).

each GONS membrane, one functionalized pore was created in its center. In the considered GONSs, the concentration of hydroxyl and epoxy groups was $C = n_o/n_c = 15\%$; where n_o is the number of oxygen atoms and n_c is the number of carbon atoms. The ratio of hydroxyl to epoxy groups was 1:1 in the GONS.

After the initial designing, the geometries optimization of functionalized GONS was calculated using DFT method. The DFT calculations were done using GAMESS at the B3LYP level of theory using 6-31G basis sets [33] to achieve their atomic charges and optimized structures. The partial charges and Lennard–Jones parameters for all atoms of simulated system are given in Table 1. The Lorentz–Berthelot mixing rules [34] were used to determine the Lennard–Jones parameters for the interactions of water–GONS, water–ion and ion–GONS.

All MD simulations for a total time of 5 ns were performed using NAMD 2.12 [35] software for 5 ns with 1 fs time step and a 12 \AA cutoff distance for the van der Waals interactions. All analyses were performed by VMD 1.9.3 [36]. Herein, the CHARMM force field was used [37] and a PME (particle mesh Ewald) method was used for long-ranged electrostatic interactions [38]. The simulation box consisted of a functionalized GONS with the size of $30 \times 30 \text{ \AA}^2$ in the middle of the box, water molecules, NaClO_4 aqueous solution and a graphene membrane as a barrier sheet at the position of $z = -40 \text{ \AA}$. The size of simulation cell was $30 \times 30 \times 80 \text{ \AA}^3$ (see Fig. 2) including 1100 water molecules and 10 perchlorate ions. For all simulations, TIP3P model [39] was used

for water molecules. The simulation box was equilibrated to minimize the energy. The system temperature was controlled at the room temperature by Langevin thermostat [40]. The membranes atoms were fixed during the simulations while water molecules and NaClO_4 were allowed to move freely.

The external pressure was applied to the systems for permeation of water molecules through the pores. For applying a hydrostatic pressure to systems, Zhu et al.'s [41, 42] technique was used. In this method, the applied pressure on water molecules was calculated by Eq. (1):

$$\Delta P = \frac{n \times F}{A}. \quad (1)$$

In this equation, ΔP is the applied pressure, n is the number of water molecules, F is a constant force which applied on the water molecules and A is the area of the box. This technique has been used in many studies of pressure-driven flow [43–47]. The hydrostatic applied pressure is in the range of 5–100 MPa. For each choice of applied pressure, the system was simulated 5–7 times with different and uncorrelated starting configurations.

The potential of the mean force (PMF) of water molecule and perchlorate ion was calculated using the umbrella sampling [48] and WHAM [49] package. This parameter can predict the passage or non-passage of water and ions through the designing pores in the membrane. Each PMF window was run for 1 ns by sampling the force experienced by the water or ions placed from -15 to 3 \AA z -positions.

Table 1 Partial atomic charges and parameters for the 12–6 Lennard–Jones potential used in the simulations

Molecule	Site	ϵ (kcal/mol)	$\sigma = R_{\min}/2$ (Å)	Charge (q)	References
GONS	Carbon bonded to epoxy group	0.069	1.907	0.1966	[29]
	Carbon bonded to hydroxyl group	0.069	1.907	0.1966	
	Oxygen in epoxy or hydroxyl	0.141	1.627	– 0.433	
	Hydroxyl hydrogen	0.000	0.000	0.352	
	Carbon bonded to hydroxyl-functionalized group in OH-pore	0.069	1.907	0.265	
	Oxygen-functionalized group in OH-pore	0.141	1.627	0.351	
	Hydrogen-functionalized group in OH-pore	0.000	0.000	– 0.605	
	Fluoride-functionalized group in F-pore	0.135	1.630	– 0.256	
	Carbon bonded to fluoride-functionalized group in F-pore	0.046	1.675	0.325	
	Hydrogen-functionalized group in H-pore	0.030	1.358	0.189	
	Carbon bonded to hydrogen-functionalized group in H-pore	0.046	1.675	– 0.181	
Graphene	Carbon	0.859	1.907	0	[57]
NaClO ₄	Sodium	0.0027	1.869	1.000	[58]
	Chloride	0.265	1.948	1.079	
	Oxygen	0.210	1.661	– 0.520	
H ₂ O	Hydrogen	0.046	0.224	0.417	[59]
	Oxygen	0.152	1.7682	– 0.834	

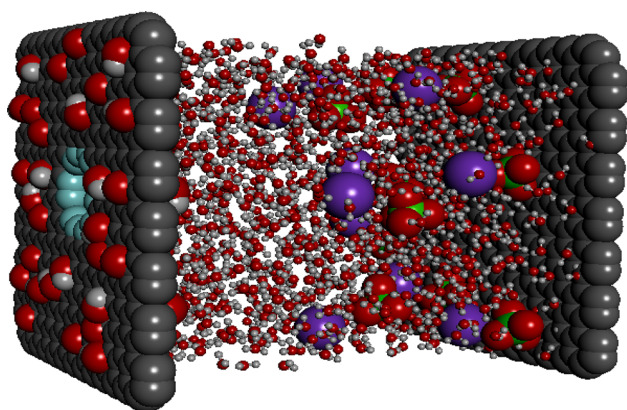


Figure 2 A schematic of the simulated box including a functionalized GONS, a graphene, water molecules and sodium perchlorate. The GONS with a fluorine-functionalized pore in its center was placed in the center of box and water molecules and ions were added to the one side of box (black: carbon, red: oxygen, white: hydrogen, green: chloride, purple: sodium and cyan: fluoride).

Results and discussion

In this research, for the separation of perchlorate ions from aqueous solution, GONS membrane was used with three types of functionalized pores with different sizes on its surface. These various functionalized pores with different sizes were chosen to study the effect of pore edge termination with functionalized group on the rate of ion separation from water. These

pores were F-pore and OH-pore as a hydrophilic pores and H-pore as a hydrophobic pore.

Water flux and PMF

The MD results showed that water molecules were able to permeate through the functionalized pores of GONS, but perchlorate ions could not pass through them, unless at high pressures. In these functionalized pores of GONS, repulsion between perchlorate ions and pore edge atoms was as a barrier to passage of perchlorate through them but this did not happen for water molecules, so that they were able to permeate the pore, because the pore diameter was suitable for their permeation. Pores of GONS were terminated by some functionalized groups on their edge. On the other hand, due to the negative charges of oxygen atoms of perchlorate, the repulsive energy was felt between them and the pore atoms. Therefore, this interaction causes perchlorate ions to be unable to pass through the functionalized pores with the exception of some cases which will be discussed later.

The water flux through various functionalized pores is shown in Fig. 3 as a function of the applied pressures. The water flux (J) is the number of water molecules permeated through the membrane pore per nanosecond [50] which is obtained by Hagen–Poiseuille's law [51, 52] as Eq. (2):

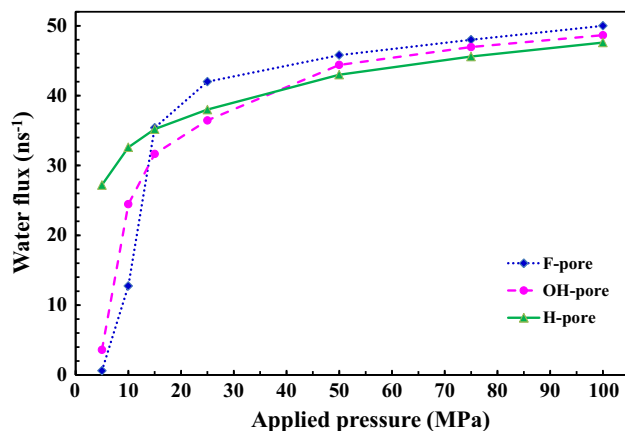


Figure 3 Water flux (ns^{-1}) as a function of applied pressure for three functionalized pores of GONS.

$$J = \frac{\Delta P \varepsilon r^2}{8 \eta l}, \quad (2)$$

where ΔP is the pressure difference, ε is the porosity, r is the pore radius, η is the viscosity and l is the membrane thickness. This equation shows the water flux increases with increasing pore radius and decreasing membrane's thickness. Accordingly, single-layer GONS with very low thickness and appropriate pores will have a high water flux.

As shown in Fig. 3, water molecules were passed through functionalized pores with different proportions. However, the trend of water flux versus pressure gradient was not linear, so that this trend has two distinct areas including low-pressure area and high-pressure area. In the low pressures, system behavior in these systems was different, so that in the F-pore and OH-pore, the amount of water flow was negligible, but in the H-pore system was significant. So, we can say, in the low pressures, the important factor is the size of pore, so that in the H-pore with largest size, the water flux was higher than all of the pores. But, in the high-pressure region, with a linear behavior change in water flux, the important factor on the water flux is the functional groups on the edge pores, so that in the hydrophilic pores (F-pore and OH-pore), water flux was more than that of hydrophobic pore (H-pore).

In the hydrophilic pores, $-\text{F}$ (fluoride) and $-\text{OH}$ (hydroxy) groups could form hydrogen bonds via water molecules which reduces the energy barrier for permeation of water molecules across them, but this phenomenon does not occur in the hydrophobic H-pore. Therefore, in the high pressures, water flux

of F-pore and OH-pore was more than H-pore. Also, according to Fig. 3, in comparison with two hydrophilic groups, the effect of F-pore in the high pressures was more than that of OH-pore and therefore water permeation through F-pore was higher than through OH-pore. Generally, it can be said that the functional groups on the pore edges of membrane have important effect on the water flux, especially at high pressures.

The results showed that the water permeability of GONS was better than of other membranes such as graphene. The obtained permeability coefficient for three investigated systems in this research agrees with other scientific works for GONS [53–55]. The permeability coefficient for the F-pore, OH-pore and H-pore systems is $591.82 \text{ L m}^{-2} \text{ h}^{-1} \text{ bar}^{-1}$, $575.84 \text{ L m}^{-2} \text{ h}^{-1} \text{ bar}^{-1}$ and $563.41 \text{ L m}^{-2} \text{ h}^{-1} \text{ bar}^{-1}$, respectively.

The trend of water flux is also confirmed with the PMF calculations. Figure 4a shows the energy barrier of water molecules when passing through the functionalized pores. As shown in Fig. 4a, the maximum amount of PMF is for the F-pore (with the least pore size) and the minimum amount is for the H-pore (with the largest pore size). With increasing pore size, the PMF was decreased; therefore, the water permeation was done easier through it. However, as shown in Fig. 3, in high-pressure region, water permeation did not depend on the pore size, but it depended on its functionalized group, so that in the higher pressures, the largest water flux was belonged to F-pore (a strong hydrophilic pore).

Also, Fig. 4b shows the PMF curves for perchlorate ion in three systems. The energy barrier for this ion was very high when it wanted to pass through the considered pores. So, permeation of perchlorate through the functionalized pores was not possible. Only at high pressures such as in the H-pore (with large pore size), some perchlorate ions passed through it due to the low energy barrier (see Fig. 4b). Of course, the ion permeation in the higher pressures through the H-pore was very low ($< 20\%$ at 100 MPa).

Density profile

The density profile of water molecules during the simulation time in the various applied pressures was obtained to study the water structure inside simulation box. As shown in Fig. 5, this parameter specifies

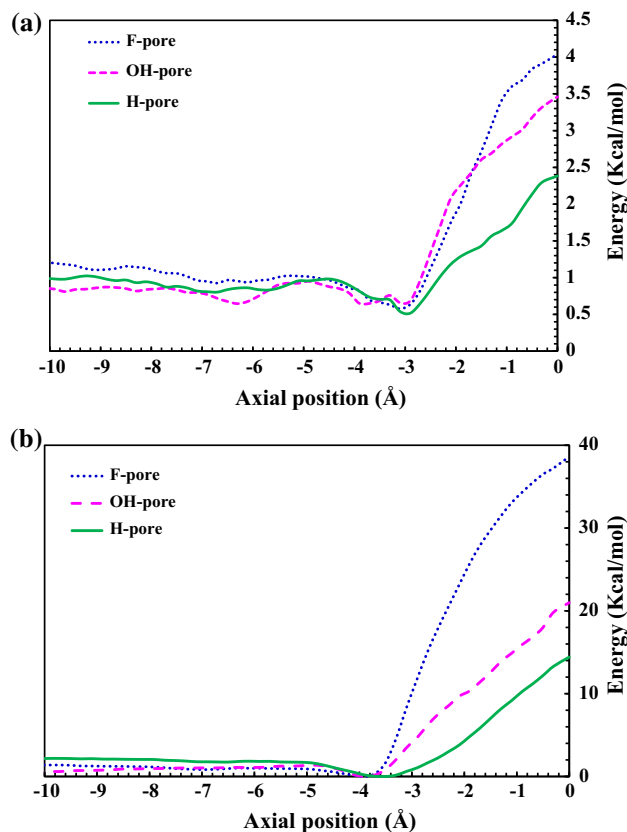


Figure 4 Potential of mean force for **a** water molecule and **b** perchlorate ions when they are trying to pass through the functionalized pores. The higher PMF values that show it face a great potential barrier when they want to pass through the pores. In these three pores, PMF values were different. Perchlorate ions faced higher energy barrier compared with water molecules.

the arrangements of water molecules in different sections of the simulated box. Due to the structure of the system, arrangement of water molecules was not the same in all parts of the simulation box. In some parts of the box, their behavior was similar to that of bulk water, but in the near membrane, water molecules behaved differently, so that they accumulate in a region within ± 3.5 Å on both sides of the GONS with two sharp peaks.

This water behavior happened in all three systems. The accumulation of water molecules near the GONS is due to the hydrogen-bonded interaction of water molecules and hydroxyl functional group on the surface of GONS and the non-bonded van der Waals interaction of water molecules and membrane atoms. In the region far away from the GONS, the water density was normal, about 1 g cm^{-3} .

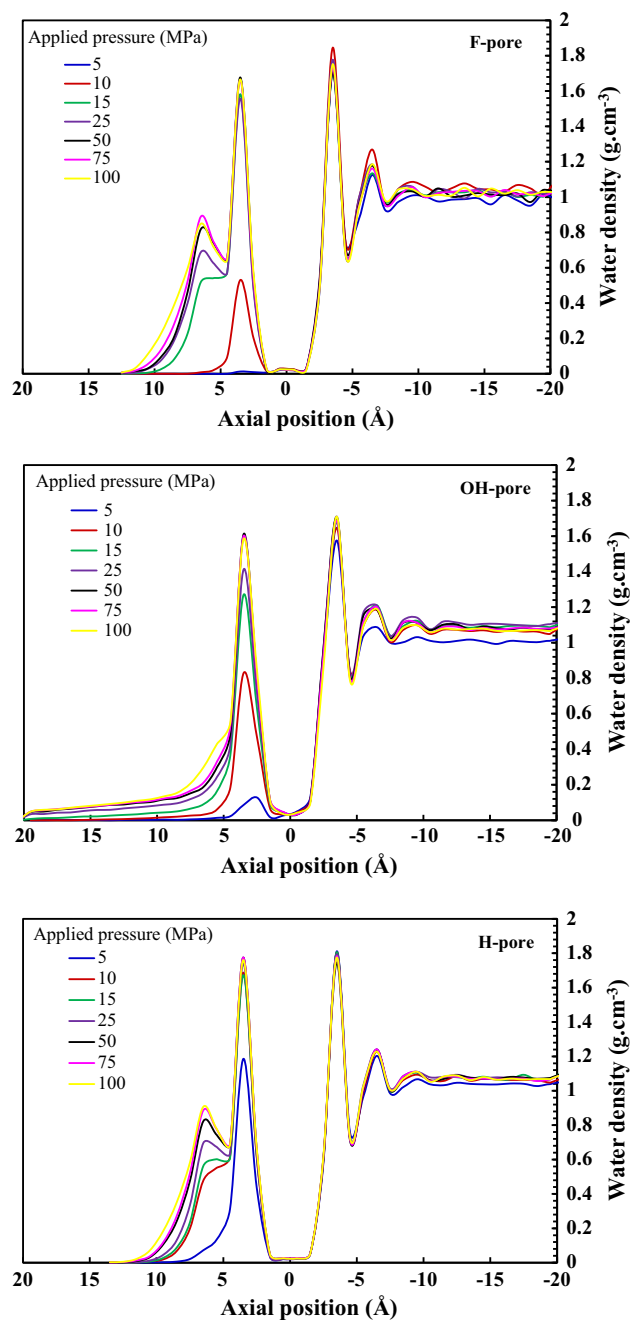


Figure 5 Density profile of water molecules in three systems. Due to the structure of the system, arrangement of water molecules was not the same in all parts of the simulation box. In some part of the box, their behavior was similar to that of bulk water, but in the near membrane, water molecules behaved differently, so that they accumulate in a region within ± 3.5 Å on both sides of the GONS with two sharp peaks.

Also, we used the radial distribution function (RDF) analysis to confirm these molecule behaviors. RDF was obtained between water molecules in a region around the GONS and also in the whole of

system in the F-pore system in 10 MPa. This trend also repeated for other systems and pressures. Figure 6 shows the RDF peak intensity of water molecules around the GONS membrane is higher than that in the whole box. This different behavior observed in RDF of water molecules is due to the accumulation of water molecules in the near GONS which their result is the formation of a layer of water molecules in this region.

Ion structure in system

Perchlorate ions were surrounded by water molecules which can be verified by their RDFs. The RDF (left axis) and integration number (right axis) of ion–water is shown in Fig. 7 for the OH-pore system. In the rest of the systems, the same trend was observed and the trend of RDF and integration number of perchlorate ions did not change much. As shown in this figure, in a short distance ($< 1.5 \text{ \AA}$), because of the repulsive forces between perchlorate and water molecules, the amount of RDF is zero. For perchlorate ion, the intensity of the RDF peaks is somewhat different for each applied pressure, and increasing the applied pressure causes the peak intensity to increase. This trend is due to higher accumulation of water molecules around perchlorate ions at the higher pressures. Also, Fig. 7 shows the integration number which is equal to the hydration number of the perchlorate ion. Integrating of $g(r)$ [56] gives the hydration number of a molecule by Eq. (3):

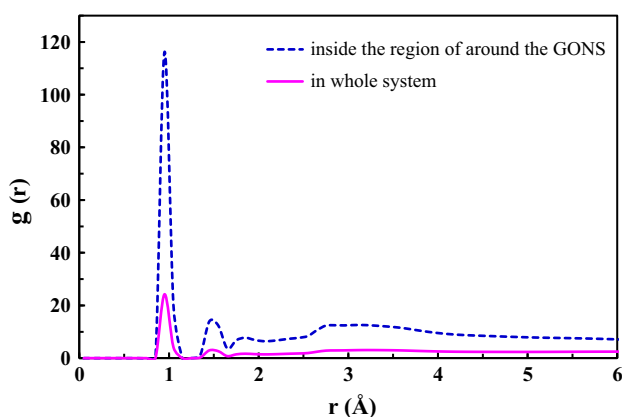


Figure 6 RDF between water molecules in a region around the GONS and also in the whole of system in F-pore system in 10 MPa. The RDF peak intensity of water molecules around the GONS membrane is higher than that of the whole box. This is due to the accumulation of water molecules in the near GONS. This trend also repeated for other systems and pressures.

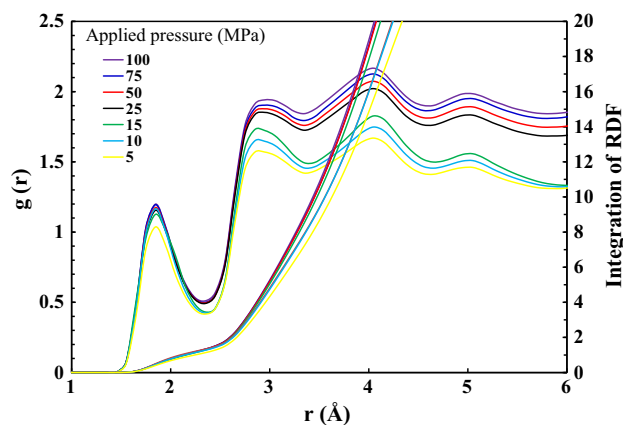


Figure 7 RDF and integration of RDF for ion–water molecules in the simulation box of OH-pore system at various applied pressures. This trend also repeated for F-pore and H-pore systems.

$$n(r) = 4\pi\rho \int_0^r g(r) \cdot r^2 \cdot dr, \quad (3)$$

in which $n(r)$, ρ , $g(r)$ and r are the hydration number, density, radial distribution function and the radial coordinate, respectively.

Hydrogen bonds

During the simulation time, when water molecules passed through the functionalized pores, hydrogen bonds were formed between water molecules and the pore edge atoms; though, this phenomenon did not occur in all systems. As shown in Fig. 8a, in the H-pore system, there is no hydrogen bond between water molecules and hydrogen atoms of edge pore. In the case of F-pore and OH-pore systems, hydrogen bonds were observed during the simulation time. At the same time, the number of hydrogen bonds did not increase significantly with increasing applied pressure. This is because a large number of water molecules were present alongside the pore edges.

So, the effective factor in this phenomenon was the type of chemical agent on the edge pore. In the F-pore and OH-pore, due to the electronegative atoms on the edge pore (fluorine and oxygen atoms), these conditions were ready for hydrogen bonds formation. On the other hands, in the OH-pore, due to the formation of hydrogen bond between the oxygen atoms of pore and hydrogen atoms of water and also between the hydrogen atoms of pore and oxygen atoms of water, the number of hydrogen bonds was highest.

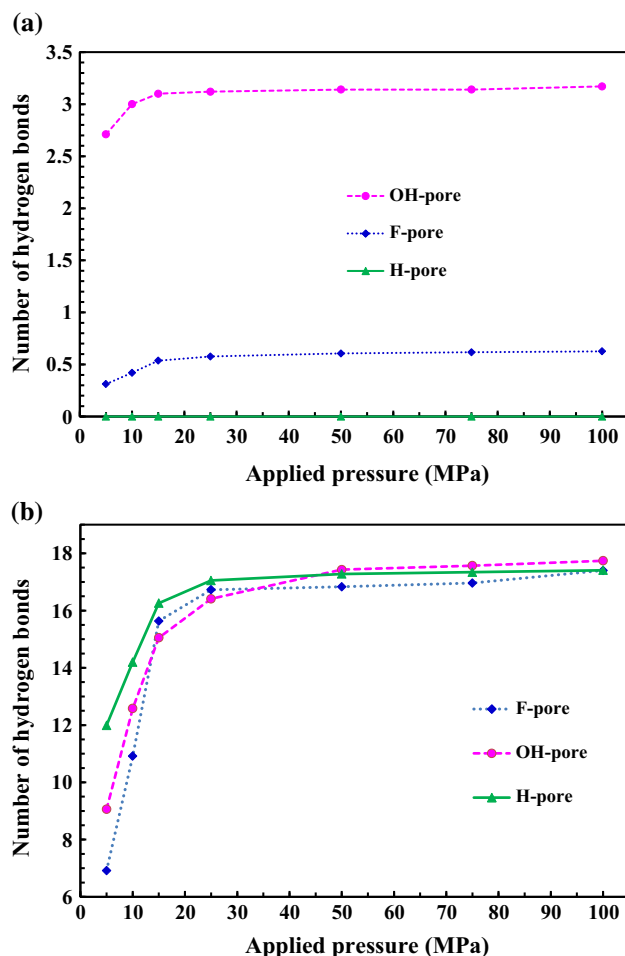


Figure 8 **a** Number of hydrogen bonds between water molecules and functionalized groups on the edge pore in various applied pressures; **b** number of hydrogen bonds between water molecules and GONS membrane in various applied pressures.

Also, we investigated the number of hydrogen bonds between water molecules and GONS membrane in various systems which is obtained by counting the hydrogen bonds during 5 ns, and their average is reported in Fig. 8b. In this case, when water molecules approach the surface of GONS membrane, hydrogen bonds were formed between them, which results in high water flux. However, due to the uniformity of the surface of GONS in all three systems, the number of hydrogen bonds did not differ significantly.

Distribution of water molecules in the simulation box was represented with the water density map in Fig. 9. The water density map was obtained with VMD by VolMap Tool. Figure 9 shows the water density map in the F-pore system in 75 MPa pressure. This VolMap shows the water molecules distributed

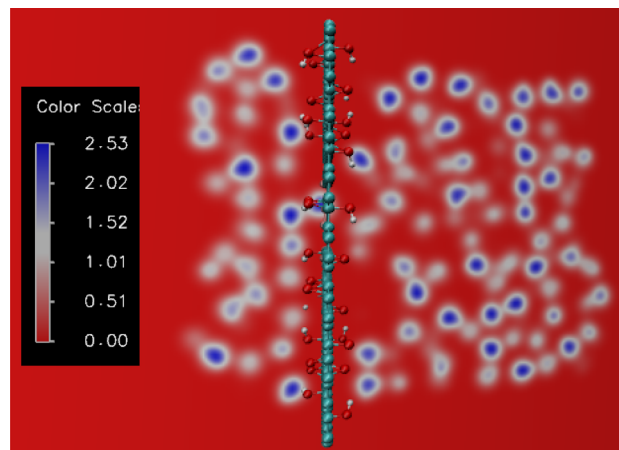


Figure 9 Water density map in the F-pore system in 75 MPa.

on the surface of membrane before and after passing through the pore of GONS. This behavior of water molecules is owing to the hydrophilic surface of GONS, which leads to high wettability property in GONS. This behavior of water molecules was repeated similarly in other systems. However, at high applied pressures, the accumulation of water molecules near the membrane was occurred more intensely.

Another important issue in the water treatment is the ability of the considered membranes for ion rejection. In our investigated systems, in all applied pressures, ion rejection by the pores of GONS with the range of from 14.65 to 24.84 Å² pore area was considered after finishing the simulation. With increasing the applied pressure and the pore size, the perchlorates rejection decreases. In the F-pore and the OH-pore systems, only at high pressures (≥ 100 MPa) ion permeation was occurred, so that at 100 MPa, near 10% of perchlorate ions were permeated from these pores (ion rejection = 90%). For the H-pore system with largest pore size, ion permeation process through this pore accelerated, so that in 75 MPa and 100 MPa ions rejection was 90% and 80%, respectively. As it can be seen, ion rejection reduced with increasing applied pressure. This is due to the fact that at the high pressures, a lot of force was applied to the ions and therefore more ions permeated through the pore [50]. In our systems, the partial charges of functional groups were acted as a barrier which it prevented the passage of perchlorate ions through pores, so that this process was desirable for separation of perchlorates from aqueous solution. This phenomenon is due to van der Waals and

electrostatic interactions between the functional groups on the edge pores and perchlorates ions. On the other hand, by applying external high pressures as a driving force to the system, some perchlorates ions can overcome these van der Waals and electrostatic interactions and therefore ions passed through pores at high pressures.

Conclusions

For efficient water treatment, GONS membranes with different functionalized pores in its center were used to separate perchlorate ions. The concentration of hydroxyl and epoxy groups in these membranes was $C = n_o/n_c = 15\%$, and the ratio of these groups was 1:1 in the GONS. For this, three types of GONS pore were functionalized with $-F$, $-OH$ and $-H$ chemical groups, immersed in an aqueous solution of sodium perchlorate. The pore sizes should be selected to have high water flux and high ion rejection. With applying external pressure to the simulation box in the range of 10–100 MPa, water molecules passed through these pores with different permeability. The obtained permeability coefficient for F-pore ($591.82 \text{ L m}^{-2}\text{h}^{-1}\text{bar}^{-1}$), OH-pore ($575.84 \text{ L m}^{-2}\text{h}^{-1}\text{bar}^{-1}$) and H-pore ($563.41 \text{ L m}^{-2}\text{h}^{-1}\text{bar}^{-1}$) showed that this functionalized nanostructure membrane can be used as a suitable membrane for water purification. The results showed that the GONS with a suitable functionalized pore was impermeable to perchlorate ions with a high permeability value for water molecules.

Acknowledgements

We thank the University of Tabriz for the support provided.

Compliance with ethical standards

Conflict of interest The authors declare no competing financial interest.

References

- [1] Iglesias A, Garrote L, Flores F, Moneo M (2007) Challenges to manage the risk of water scarcity and climate change in the Mediterranean. *Water Resour Manage* 21:775–788
- [2] Vasudevan S, Oturan MA (2014) Electrochemistry: as cause and cure in water pollution—an overview. *Environ Chem Lett* 12:97–108
- [3] Van der Bruggen B, Vandecasteele C (2003) Removal of pollutants from surface water and groundwater by nanofiltration: overview of possible applications in the drinking water industry. *Environ Pollut* 122:435–445
- [4] Motzer WE (2001) Perchlorate: problems, detection, and solutions. *Environ Forensics* 2:301–311
- [5] Nzungung VA, Wang C (2012) Perchlorate-contaminated water. *Perchlorate Environ* 57:219–229
- [6] Kannan K, Praamsma ML, Oldi JF, Kunisue T, Sinha RK (2009) Occurrence of perchlorate in drinking water, groundwater, surface water and human saliva from India. *Chemosphere* 76:22–26
- [7] Damtie MM, Kim B, Woo YC, Choi J-S (2018) Membrane distillation for industrial wastewater treatment: studying the effects of membrane parameters on the wetting performance. *Chemosphere* 206:793–801
- [8] Curteanu S, Piuleac CG, Godini K, Azaryan G (2011) Modeling of electrolysis process in wastewater treatment using different types of neural networks. *Chem Eng J* 172:267–276
- [9] Singh N, Nagpal G, Agrawal S (2018) Water purification by using adsorbents: a review. *Environ Technol Innov* 11: 187–240. <https://doi.org/10.1016/j.eti.2018.05.006>
- [10] Luo T, Abdu S, Wessling M (2018) Selectivity of ion exchange membranes: a review. *J Membr Sci* 555:429–454. <https://doi.org/10.1016/j.memsci.2018.03.051>
- [11] Bunani S, Yörükoğlu E, Yüksel Ü, Kabay N, Yüksel M, Sert G (2015) Application of reverse osmosis for reuse of secondary treated urban wastewater in agricultural irrigation. *Desalination* 364:68–74
- [12] Henze M, Harremoës P, la Cour JJ, Arvin E (2001) *Wastewater treatment: biological and chemical processes*. Springer, Berlin
- [13] Sadik OA, Du N, Yazgan I, Okello V (2014) *Nanotechnology applications for clean water*, 2nd edn. Elsevier, Amsterdam
- [14] Kanchi S (2014) Nanotechnology for water treatment. *J Environ Anal Chem* 1:1–3
- [15] Song X, Guo H, Tao J, Zhao S, Han X, Liu H (2018) Design of tunable-size 2D nanopore membranes from self-assembled amphiphilic nanosheets using dissipative particle dynamics simulations. *Chem Eng Sci*. <https://doi.org/10.1016/j.ces.2018.05.023>
- [16] Das R, Ali ME, Hamid SBA, Ramakrishna S, Chowdhury ZZ (2014) Carbon nanotube membranes for water purification: a bright future in water desalination. *Desalination* 336:97–109

- [17] Golberg D, Bando Y, Huang Y et al (2010) Boron nitride nanotubes and nanosheets. *ACS Nano* 4:2979–2993. <http://doi.org/10.1021/nn1006495>
- [18] Azamat J, Khataee A, Joo SW (2014) Functionalized graphene as a nanostructured membrane for removal of copper and mercury from aqueous solution: a molecular dynamics simulation study. *J Mol Graph Model* 53:112–117
- [19] Jahanshahi D, Vahid B, Azamat J (2018) Computational study on the ability of functionalized graphene nanosheet for nitrate removal from water. *Chem Phys* 511:20–26. <https://doi.org/10.1016/j.chemphys.2018.05.018>
- [20] Rikhtehgaran S, Lohrasebi A (2018) Multilayer nanoporous graphene as a water purification membrane. *J Nanosci Nanotechnol* 18:5799–5803
- [21] Nair R, Wu H, Jayaram P, Grigorieva I, Geim A (2012) Unimpeded permeation of water through helium-leak-tight graphene-based membranes. *Science* 335:442–444
- [22] Yu T, Xu Z, Liu S, Liu H, Yang X (2018) Enhanced hydrophilicity and water-permeating of functionalized graphene-oxide nanopores: molecular dynamics simulations. *J Membr Sci* 550:510–517
- [23] Cohen-Tanugi D, Grossman JC (2012) Water desalination across nanoporous graphene. *Nano Lett* 12:3602–3608. <https://doi.org/10.1021/nl3012853>
- [24] Wang Y, Sinha S, Ahuja K et al (2018) Dynamics of a water nanodrop through a holey graphene matrix: role of surface functionalization, capillarity, and applied forcing. *J Phys Chem C*. <https://doi.org/10.1021/acs.jpcc.8b01749>
- [25] Liu Y, Liu H (2018) Time-dependent density functional theory for fluid diffusion in graphene oxide membranes/graphene membranes. *Chem Eng Sci* 188:150–157. <https://doi.org/10.1016/j.ces.2018.05.010>
- [26] Dikin DA, Stankovich S, Zimney EJ et al (2007) Preparation and characterization of graphene oxide paper. *Nature* 448:457–460
- [27] Li H, Song Z, Zhang X et al (2013) Ultrathin, molecular-sieving graphene oxide membranes for selective hydrogen separation. *Science* 342:95–98
- [28] Lin L-C, Grossman JC (2015) Atomistic understandings of reduced graphene oxide as an ultrathin-film nanoporous membrane for separations. *Nat Commun* 6:8335. <https://doi.org/10.1038/ncomms9335>. <http://www.nature.com/articles/ncomms9335#supplementary-information>
- [29] Wei N, Peng X, Xu Z (2014) Understanding water permeation in graphene oxide membranes. *ACS Appl Mater Interfaces* 6:5877–5883. <https://doi.org/10.1021/am500777b>
- [30] Shi K, Lian C, Bai Z, Zhao S, Liu H (2015) Dissipative particle dynamics study of the water/benzene/caprolactam system in the absence or presence of non-ionic surfactants. *Chem Eng Sci* 122:185–196
- [31] Song X, Zhao S, Fang S, Ma Y, Duan M (2016) Mesoscopic simulations of adsorption and association of PEO-PPO-PEO triblock copolymers on a hydrophobic surface: from mushroom hemisphere to rectangle brush. *Langmuir* 32:11375–11385
- [32] Ebro H, Kim YM, Kim JH (2013) Molecular dynamics simulations in membrane-based water treatment processes: a systematic overview. *J Membr Sci* 438:112–125. <https://doi.org/10.1016/j.memsci.2013.03.027>
- [33] Schmidt MW, Baldrige KK, Boatz JA et al (1993) General atomic and molecular electronic structure system. *J Comput Chem* 14:1347–1363
- [34] Nath SK (2003) Molecular simulation of vapor-liquid phase equilibria of hydrogen sulfide and its mixtures with alkanes. *J Phys Chem B* 107:9498–9504. <https://doi.org/10.1021/jp034140h>
- [35] Phillips JC, Braun R, Wang W et al (2005) Scalable molecular dynamics with NAMD. *J Comput Chem* 26:1781–1802
- [36] Humphrey W, Dalke A, Schulten K (1996) VMD: visual molecular dynamics. *J Mol Graph* 14:33–38
- [37] MacKerell A, Bashford D, Bellott M, Joseph-McCarthy D, Kuchnir L, Kuczera K, Lau FTK, Mattos C, Michnick S, Ngo T, Nguyen DT, Prodhom B, Reiher WE, Roux B, Schlenkrich M, Smith JC, Stote R, Straub J, Watanabe M, Wiór-kiewicz-Kuczera J, Yin D, Karplus M et al (1998) All-atom empirical potential for molecular modeling and dynamics studies of proteins. *J Phys Chem B* 102:3586–3616
- [38] Song X, Guo H, Tao J, Zhao S, Han X, Liu H (2018) Encapsulation of single-walled carbon nanotubes with asymmetric pyrenyl-gemini surfactants. *Chem Eng Sci* 187:406–414
- [39] Jorgensen WL, Chandrasekhar J, Madura JD, Impey RW, Klein ML (1983) Comparison of simple potential functions for simulating liquid water. *J Chem Phys* 79:926–935. <https://doi.org/10.1063/1.445869>
- [40] Wu G, Robertson DH, Brooks CL, Vieth M (2003) Detailed analysis of grid-based molecular docking: a case study of CDOCKER—A CHARMM-based MD docking algorithm. *J Comput Chem* 24:1549–1562
- [41] Zhu F, Tajkhorshid E, Schulten K (2002) Pressure-induced water transport in membrane channels studied by molecular dynamics. *Biophys J* 83:154–160. [https://doi.org/10.1016/S0006-3495\(02\)75157-6](https://doi.org/10.1016/S0006-3495(02)75157-6)
- [42] Zhu F, Tajkhorshid E, Schulten K (2004) Theory and simulation of water permeation in aquaporin-1. *Biophys J* 86:50–57. [https://doi.org/10.1016/S0006-3495\(04\)74082-5](https://doi.org/10.1016/S0006-3495(04)74082-5)
- [43] Azamat J, Khataee A, Joo SW (2015) Molecular dynamics simulation of trihalomethanes separation from water by

- functionalized nanoporous graphene under induced pressure. *Chem Eng Sci* 127:285–292. <https://doi.org/10.1016/j.ces.2015.01.048>
- [44] Corry B (2008) Designing carbon nanotube membranes for efficient water desalination. *J Phys Chem B* 112:1427–1434. <https://doi.org/10.1021/jp709845u>
- [45] Azamat J, Sardroodi JJ, Mansouri K, Poursoltani L (2016) Molecular dynamics simulation of transport of water/DMSO and water/acetone mixtures through boron nitride nanotube. *Fluid Phase Equilib* 425:230–236
- [46] Wang Y, He Z, Gupta KM, Shi Q, Lu R (2017) Molecular dynamics study on water desalination through functionalized nanoporous graphene. *Carbon* 116:120–127. <https://doi.org/10.1016/j.carbon.2017.01.099>
- [47] Trung KH, Bo L, Kun Z, Wing-Keung LA (2017) Pressure-driven water permeation through multilayer graphene nanosheets. *Physica Status Solidi (b)* 254:1700074. <https://doi.org/10.1002/pssb.201700074>
- [48] Torrie GM, Valleau JP (1977) Nonphysical sampling distributions in Monte Carlo free-energy estimation: umbrella sampling. *J Comput Phys* 23:187–199
- [49] Roux B (1995) The calculation of the potential of mean force using computer simulations. *Comput Phys Commun* 91:275–282. [https://doi.org/10.1016/0010-4655\(95\)00053-I](https://doi.org/10.1016/0010-4655(95)00053-I)
- [50] Heiranian M, Farimani AB, Aluru NR (2015) Water desalination with a single-layer MoS₂ nanopore. *Nat Commun* 6:8616. <https://doi.org/10.1038/ncomms9616>
- [51] Baker RW (2012) *Membrane technology and applications*. Wiley, Chichester
- [52] Werber JR, Osuji CO, Elimelech M (2016) Materials for next-generation desalination and water purification membranes. *Nat Rev Mater* 1:16018. <https://doi.org/10.1038/natrevmats.2016.18>
- [53] Boukhvalov DW, Katsnelson MI, Son Y-W (2013) Origin of anomalous water permeation through graphene oxide membrane. *Nano Lett* 13:3930–3935. <https://doi.org/10.1021/nl4020292>
- [54] Liang H, Yingru L, Qinqin Z, Wenjing Y, Gaoquan S (2015) Graphene oxide membranes with tunable semipermeability in organic solvents. *Adv Mater* 27:3797–3802. <https://doi.org/10.1002/adma.201500975>
- [55] Zhang Y, Chung T-S (2017) Graphene oxide membranes for nanofiltration. *Curr Opin Chem Eng* 16:9–15. <https://doi.org/10.1016/j.coche.2017.03.002>
- [56] Duan M, Song X, Zhao S et al (2017) Layer-by-layer assembled film of asphaltenes/polyacrylamide and its stability of water-in-oil emulsions: a combined experimental and simulation study. *J Phys Chem C* 121:4332–4342
- [57] Beu TA (2010) Molecular dynamics simulations of ion transport through carbon nanotubes. I. Influence of geometry, ion specificity, and many-body interactions. *J Chem Phys* 132:164513. <https://doi.org/10.1063/1.3387972>
- [58] Nieszporek K, Nieszporek J, Trojak M (2016) Calculations of shear viscosity, electric conductivity and diffusion coefficients of aqueous sodium perchlorate solutions from molecular dynamics simulations. *Comput Theor Chem* 1090:52–57. <https://doi.org/10.1016/j.comptc.2016.06.002>
- [59] Price DJ, Brooks CL (2004) A modified TIP3P water potential for simulation with Ewald summation. *J Chem Phys* 121:10096. <https://doi.org/10.1063/1.1808117>